THE INVESTIGATION OF ALTERNATIVE SOLID PROPELLANTS IN HALL THRUSTERS

Vlad-George Tirila[(1)], Ashley Hallock [(2)], Alain Demairé [(3)], Charlie Ryan [(4)]

[(1)] *University of Southampton, Southampton SO171 BJ (United Kingdom), Email: v-g.tirila@soton.ac.uk*
[(2)] *OHB Sweden, OHB Sweden AB, SE-164 29 Kista* (Sweden)*, Email: ashley.hallock@ohb-sweden.se*
[(3)] *OHB Sweden, OHB Sweden AB, SE-164 29 Kista* (Sweden)*, Email: alain.demaire@ohb-sweden.se*
[(4)] *University of Southampton, Southampton SO171BJ (United Kingdom), Email: c.n.ryan@soton.ac.uk*

KEYWORDS: alternative propellants, metallic propellants, new propellants, zinc, sublimation, electric propulsion, propellant storage and delivery system, PSDS, Hall thruster

ABSTRACT:

While the high price of xenon makes it a significant fraction of the satellite cost [1], the superior performance of xenon offsets the additional cost compared to other gaseous propellants. However, solid propellants could be an attractive alternative due to their low cost, compact storage and ease of handling. Zinc and magnesium have shown potential for high performance in electric propulsion [2]. In the work presented here these propellants are further explored experimentally for usage in Hall thrusters. A propellant storage and delivery system for metallic propellants has been designed, built and operated with zinc propellant. Flow rates of 0.5 to 6.09 SCCM (0.0243 mg/s to 0.2961 mg/s) were measured at a heater power input ranging from 40 W to 110 W. The results were compared with theoretical data [3] showing good agreement and an efficiency factor for the heating method was calculated to be $\eta = 0.7$.

1. INTRODUCTION

This investigation of alternative Hall thruster propellants is an ongoing three-year project supported by the University of Southampton and OHB Sweden. The goal of the project is to design, develop and test a propellant storage and delivery system (PSDS) that can be used with a variety of solid propellants in a Hall thruster. The preliminary results of the first part of the project are presented in this paper and include the development of a controllable and energy efficient PSDS for zinc.

1.1. Motivation

Currently, xenon is the most prevalent propellant among electric propulsion (EP) subsystems [4]. Major benefits such as the relatively high atomic mass, inert nature, large ionization cross section and the lowest first ionization potential amongst the stable noble gases come at the cost of the parasitic mass of the supercritical storage and delivery infrastructure. High pressure tanks, distribution systems and temperature control are unavoidable [5]. Further, the high cost incurred by limited production capacity and usage across multiple industrial branches make it a volatile commodity under the constraints of the market [1]. Krypton has a lower cost (estimated currently at 1/10 of xenon). Due to a lower atomic mass, a 25% increase in specific impulse (assuming no losses) is expected in a direct comparison with xenon [6]. Moreover, krypton usage requires a minimalistic redesign of the distribution system for a Hall thruster PSDS that utilizes xenon. However, compared to xenon, usage of krypton leads to a reduction in thrust efficiency due to a higher ionization potential, smaller ionization cross section and a mass penalty due to higher pressure requirements for storage [6] coupled with a very low density even under pressure (1/3 of the xenon value). A higher beam divergence has been measured for Hall thrusters operating on argon and nitrogen compared to the expected value for xenon at an equivalent discharge voltage and propellant flow rate. Voltage discharge is not significantly reduced leading to a lower propellant efficiency compared to xenon [7]. The various drawbacks in terms of efficiency, storage density or cost of the gaseous alternative propellants has motivated exploring the feasibility of solid elements.

1.2. Solid Propellants

The variation in physical properties of the solid propellants discussed herein enable tailoring of the propulsion system to a specific budget, mission, or operational performance profile. A discussion of the advantages and disadvantages of iodine, bismuth, zinc, and magnesium (as alternative propellants to xenon) follows. Other elements including caesium, lithium and cadmium have also been evaluated as alternative propellants and a discussion of their advantages and disadvantages can be found in the literature [8].

The properties of iodine and xenon are similar both in terms of atomic mass and first ionization energy, but due to its solid form, iodine can be stored with a density 3 times that of xenon. The low melting temperature of 113.7º C, up to which high vapor pressures can be obtained [5], is also beneficial due to the low power input required to phase transition the solid iodine to a vapor through sublimation. The major drawback of iodine is the reactivity of the element and its subsequent interaction with other subsystems, a topic of ongoing research [8][9].

Bismuth has a much heavier atom than xenon. This results in increased thrust and propellant utilization efficiency with one of the highest achievable thrust to discharge power ratios (T/P). However, a major disadvantage is the high temperature required to achieve a sufficiently high vapor pressure along with the need to pre-heat and maintain contact surfaces above 700º C to prevent condensation [8][10] Due to the inherent difficulty associated with operation at high temperature, controllability and start-up [11], bismuth is deemed more suited towards higher power thrusters in the kW range and larger missions that can benefit more from the T/P ratio in the order of 70 – 80 (mN/kW) and higher [10][12].

Magnesium is one of the lightest solid elements proposed as an alternative propellant. A low atomic mass leads to high values of specific impulse reaching over 4000s [8] in theoretical predictions at a discharge of 275 V. The low ionization energy and large ionization cross section are also desirable properties when considering the ease of ionization. Storage density (1.738 g/cm^3) is higher although only marginally compared to xenon at a supercritical state (1.598 g/cm^3). Unlike bismuth, a high vapor pressure can be achieved at lower temperatures, as low as 440º C. Considering the potential performance possible at a relatively low discharge voltage and the heater power requirements, magnesium is an attractive option for small to large thrusters [13].

Zinc is a similarly light element with an atomic mass half that of a xenon atom, with a lower ionization energy and comparable ionization cross section. The main advantages of zinc are in its storage density, almost 4.5 times higher than xenon, and low sublimation temperature, with sufficient vapor pressures being achieved above 300º C. Further, unlike magnesium, it is a benign element that is not reactive and can be machined easily and procured at a much lower cost than xenon.

While all solid propellants offer several advantages compared to gaseous propellants, most notably a reduced subsystem mass and complexity, the TRL (technology readiness level) of solid propellants remains low, in part due to a paucity of EP thruster performance data. The goal of this project is to contribute to the development of solid EP propellants by designing and building a Hall thruster module, including a built-in propellant storage and delivery system, capable of operation on solid propellants, demonstrating the performance of this thruster numerically (through kinetic particle-in-cell simulations), and finally by confirming the numerical predictions through direct performance measurements of thruster operation on zinc and magnesium.

2. DESIGN OF THE ZINC PROPELLANT DELIVERY SYSTEM

A solid propellant must undergo a phase transition to allow for ionization and subsequent acceleration by a Hall thruster with a conventional design. This can be achieved through a liquid transition or by exploiting the sublimation phenomenon that occurs at low pressure.

Several propellant delivery systems have been developed for alternative propellants. Most rely on a reservoir of liquid metal heated externally outside the thruster for which gas is delivered via a heated propellant feed line [5]. Other designs use a heating element in direct contact with the solid propellant, forcing a localized phase transition that includes a transition to the liquid state [10],[4]. Alternatively, the anode itself can be replaced in a Hall thruster with a multi layered structure housing liquid metal with a high porosity filter for gas distribution. Furthermore, the anode can be made entirely out of the propellant metal and the residual discharge heat can be used to sublimate the needed quantity and sustain the reaction [14]. This represents an elegant solution to the problem of energy efficiency however, the amount of propellant is limited by the volume of the anode. Moreover, the main difficulty lies in the control system required to maintain the reaction since changing the characteristics of the discharge has a cascading effect on the sublimation rate which further alters the electric discharge [15]. While the propellant storage and delivery system (PSDS) design is also affected by the selected propellant species, the available power, the required flow rate and the vapor pressure required to achieve this flow rate, sublimation is generally preferred due to the complexity and power requirements of storing and maintaining a liquid metal propellant [16]. Considering that a goal of the present project is to develop a PSDS for lower-power (200-500 W) Hall thrusters, zinc sublimation was chosen as an appropriate solid propellant delivery method. To the authors knowledge, the presented PSDS represents a novel design which makes use of direct sublimation of zinc rather than localized melting. Furthermore, the PSDS can use most alternative propellants that can achieve a good vapor pressure bellow their melting point up to the temperature limit of the heater. Planned future work includes development of a PSDS capable of operation without feed line heaters in an improved, direct-distribution design.

2.1. Flow Rate Control

Though liquid propellant storage offers the advantage of thermal stability, a transition through the boiling point is avoided in the present PSDS design due to the higher temperature and energy requirements of liquid propellant storage and the limited available power in the targeted satellite platforms. Instead, a solid propellant is maintained at a low ambient pressure and directly transitioned to a gaseous state by gradually increasing the temperature until the target gas flow rate is achieved. Precise control of the flow rate for this type of PSDS requires precise temperature regulation. The dependency between available mass flow rate at a specific slug surface area and temperature is needed both for an optimum design and for the adequate operation of the PSDS. Since flow controllers are avoided due to the high temperature required by zinc and magnesium, a theoretical investigation aids in the construction of an empirical map that associates a heating mode to a mass flow rate. A functional dependency between propellant temperature and the resulting propellant flow rate is derived below.

Assuming a perfect vacuum, the Hertz-Knudsen equation provides a starting point to determine the flow rate of a vapor from a solid surface [15] and can be written as:

$$\dot{m} = \frac{P_v(T_s)}{\sqrt{\frac{2\pi k_B T_s}{M}}}\, A \qquad (1)$$

where P_v represents the vapor pressure of the element comprising the solid surface (Pa), k_B the Boltzmann constant, T_s the temperature of the solid surface (K), M the molecular mass of the element comprising the solid surface in kg and A the exposed area of the solid surface (m^2). Eq. 1 is used in literature to describe both evaporation as well as sublimation and is presented in its simplest form for practical use. The equation must be modified to account for several inefficiencies. Firstly, outside of a perfect vacuum assumption, a small pressure component exists (P_c chamber pressure). A vapor cloud will be present above the solid surface of the slug promoting collisions and hence a backscatter of zinc particles which condense on the surface of the slug. Thus, a reduction in the effective value of the mass flow rate off the solid surface must be accounted.

Secondly, the surface quality of the slug can affect the sublimation rate. The presence of oxidation or a pitting pattern can either inhibit or promote sublimation. A term η is introduced as a semi-empirical parameter to account for physical variations among PSDS designs.

The mean free path λ becomes a critical parameter in characterizing the type of sublimation [17]:

$$\lambda = \frac{k_B T}{\sqrt{2}\pi d^2 P} \qquad (2)$$

Where k_B is the Boltzmann constant, T is the soaking temperature in K, d the diameter of the zinc atom in m (1.39×10^{-10} m) and P the vacuum pressure in Pa. At $T = 300^0$ C and $P = 0.1\ Pa$ for a zinc atom, $\lambda = 0.23$ m. In the PSDS design it is important to consider characteristic lengths such as the length of the feed line or the distance between the slug and walls to be smaller than the mean free path as to promote a molecular flow reducing collisional losses and subsequent condensation back onto the zinc slug. In the case of the feed line, a short, direct path to the discharge chamber bellow the mean free path ensures minimal collisions and reduces the likelihood of deposition onto the feed line inner surfaces without the need of an external heater.

To estimate a theoretical mass flow rate, the vapor pressure must first be calculated. The rate of vapor pressure build-up specific to the element (P_v) with increasing temperature is described using the following relationship for metallic elements derived by C. Alcock [3]:

$$\log(P_v) = 5.006 + A + B + T^{-1} + \\ +C\ log(T) + DT^{-3} \qquad (3)$$

Where A, B, C and D are empirical coefficients specific to zinc in solid form. Alternatively, the Clausius-Clapeyron relation can be used [18]:

$$P_v = P_{ref} e^{-\frac{\Delta h_s}{R}\left(\frac{1}{T_1} - \frac{1}{T_{ref}}\right)} \qquad (4)$$

Where P_{ref} and T_{ref} represent reference values chosen along the phase curve and Δh_s represents the latent heat of sublimation for zinc.

Finally, the chamber pressure can be introduced in Equation 1 along with η, representing the discussed losses, and the resulting sublimation mass flow rate off the solid slug follows the following formula:

$$\dot{m} = \eta \frac{P_v(T_s) - P_c}{\sqrt{\frac{2\pi k_B T_s}{M}}}\, A \qquad (5)$$

Converting kg/s to SCCM for zinc gives the following result ($1SCCM = 4.477962 \times 10^{17} M\dot{m}$):

$$\dot{m} = \eta \frac{P_v(T_s) - P_c}{4.477962 \times 10^{17} \sqrt{2\pi M k_B T_s}}\, A \qquad (6)$$

The vapor pressure for both zinc and magnesium in

a comparison between the two methods stated can be found in Figure 1. In the case of zinc, the Clausius-Clapeyron curve matches perfectly the equation written by C. Alcock (Equation 3 and 4) with a larger discrepancy seen in the case of magnesium. The melting point temperature represents the operational limit for a sublimation PSDS with a theoretical limit of $P_v = 22\ Pa$ for zinc close to the melting point and $P_v = 380\ Pa$ for magnesium. The resulting vapor pressure for both elements can drive sufficient propellant flow even for high-power electric thrusters.

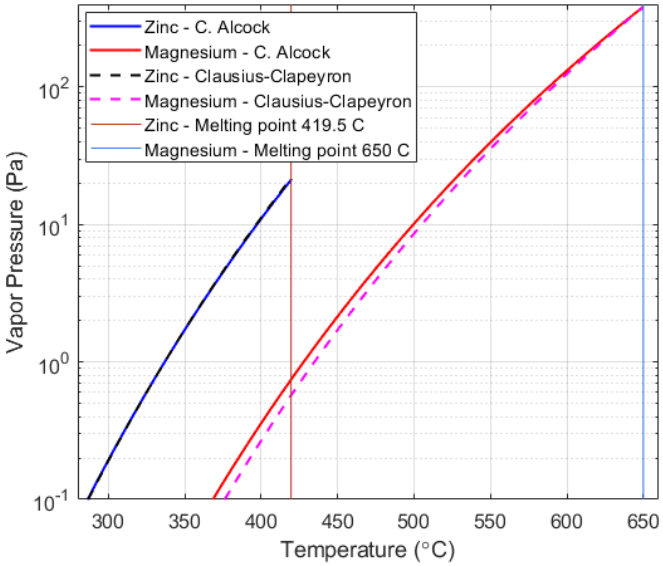

Figure 1: Vapor pressure (P_v) vs temperature (T) for zinc and magnesium up to the melting point

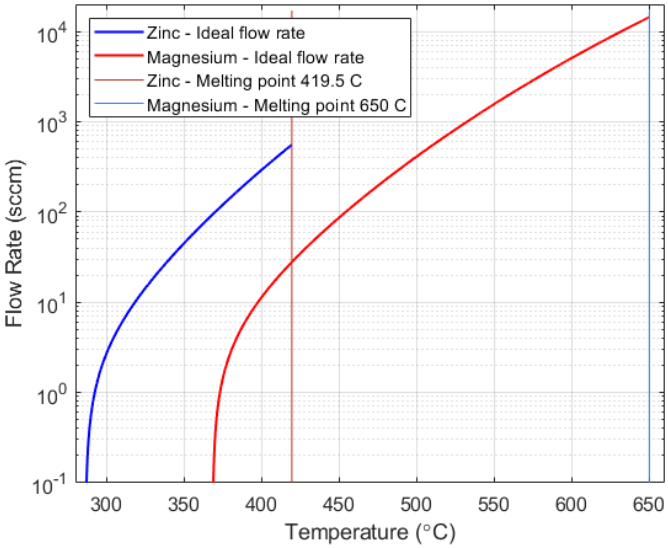

Figure 2: Flow rate ($\dot{m}$) vs temperature (T) for zinc and magnesium up to the melting point. $P_c = 0.1\ Pa$

For alternative propellants testing, the diffusion pump that is equipped to the vacuum chamber can achieve pressures as low as $P_c = 0.001\ Pa$ when no gas is being produced or injected. Accounting for the zinc output from the PSDS during operation, a sustainable working pressure of $P_c = 0.1\ Pa$ was chosen for this demonstration. The theoretical ideal flow rates are shown in Figure 2 where $\eta = 1$ (Equation 5) for a zinc slug which has an outer radius $r = 8$ mm and a height $h = 19$ mm. In this case, the side area of the cylinder is used. Theoretical flow rates of up to 480 SCCM (23.335 mg/s) are possible with zinc and much higher ones for magnesium proving again the propellant viability for larger thruster usage. Flow rates of up to 10 SCCM (0.486 mg/s) are achievable close to 320^0 C for zinc and 398^0 C for magnesium suggesting a relative low power input (achievable with a 110 W heater). These flow rates fit the operational profile of a small Hall thruster in the 200-500 W range. However, precise control is needed to maintain the flow rate at a set value. Variations of up to 1^0 C can change the flow rate by 0.5 SCCM (0.024 mg/s), and therefore precise thermal control is critical to be able to deliver the correct flow rate as required by the receiving Hall thruster.

2.2. Condensation Considerations

Once the solid propellant transitions to the gaseous state, any surfaces with which the propellant can come into contact must be held at temperatures well above the typical temperature range of a satellite environment to avoid condensation. If the gaseous propellant loses too much energy it can lead to crystalline formations on the feed lines or the tank walls, causing obstructions to the propellant flow. Recommendations in the literature are limited with regards to preventing condensation on critical components, however investigations [4],[5],[12] of iodine and bismuth indicate that the wetted surfaces should be maintained above the setpoint sublimation temperature of the propellant to ensure direct evaporation should a collision occur. Although this a viable approach to preventing blockage, the higher temperature required would put a strain on the power supply subsystem in case of larger propellant tanks. This project aims to provide an improved solution, to reduce and optimize the energy required by the PSDS by firstly analysing the condensation behaviour in this experiment and incorporating adjustments to the third iteration of the PSDS.

2.3. PSDS Design

It has previously been demonstrated that zinc flowrates up to 15.5 SCCM (0.753 mg/s) and propellant flow durations up to 80 minutes are achievable with a PSDS based on sublimation and solid zinc storage [19]. The goal of the present PSDS design is to improve upon this previous design by increasing the heat transfer efficiency from the heaters to the propellant, thereby

decreasing the required heater power, the ambient temperature in the vacuum chamber and the uncertainty of the mass flow rate control.

A single, 110 W cartridge heater with a diameter of 6.35 mm was used to heat up an annular slug of zinc from the centre. The slug measures 19 mm in height and is 16 mm in diameter with a mass of 22.25 grams. The relatively high thermal conductivity of zinc (112.2 W/mK) compared to other solid propellants such as iodine and bismuth allows a fast response from the controller and subsequently a high temperature stability, with oscillations dampened by the bulk of the material. The side area of the slug was exposed to promote a high mass flow rate with a lower energy input. Since the heater is at the core of the metallic slug, heat expansion of the heater contact surface coupled with the heat expansion of the zinc slug inner surface ensures adequate surface contact and conduction as the two are pushed together. Furthermore, the mass of zinc acts as a thermal damper, flattening any oscillations in temperatures from the heater on and off cycle. The assembly is enclosed in a stainless-steel cylinder measuring 30 mm in diameter and leads via a feed line measuring 22.25 mm in length to the anode. A threaded cap was used to access and replace the zinc slug and heater. As the slug radiates outwards, it passively contributes to the heating of the walls reducing radiative losses. A CAD of the cross-section of the prototype with the components labelled is shown in Figure 3. A photograph of the assembly can be seen in Figure 4. The PSDS is designed to be connected with sufficient thermal conduction to an anode equipped with its own heater such that the anode heater would contribute to heating of the feed line and tank walls.

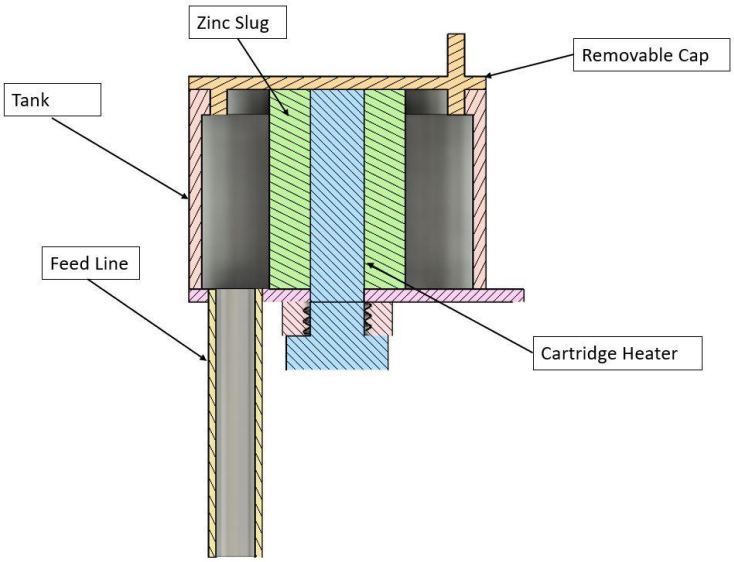

Figure 3: Proposed tank design – section view; zinc slug (green); cartridge heater (blue)

Figure 4: Propellant tank, cartridge heaters and anode assembly on ceramic mount

Cartridge heaters with built-in, calibrated thermocouples were used to improve the precision of the temperature control compared to previous PSDS designs [19]. Since these heaters come in a wide range of sizes and powers (reaching temperatures of up to 750^{0}C) this PSDS design can accommodate a wide range of propellant masses of not only zinc but other propellants such as magnesium and even iodine. Therefore, this PSDS design can easily be tailored for a wide range of mission profiles.

3. DESCRIPTION OF THE EXPERIMENT

The equipment used for testing this PSDS design is described in this section. A description of the control system, support mount and vacuum chamber facilities can be found in [19].

3.1. Thermal Control System

The two 110 W cartridge heaters were powered at 110 V AC and a feedback loop was established with the built-in J-type thermocouples. In addition, secondary thermocouples were used for the calibration process and for backup measurements during the experiment. The initial setup featured a simple ON/OFF switch with a manual variac for changing the input voltage [12]. The control system used in [19] was employed for these tests. A schematic of the control system is shown in Figure 5.

3.2. Vacuum Chamber

The tests described in the paper were performed in a small vacuum chamber with a diameter of 40 cm and length of 70 cm equipped with a roughing pump and a diffusion pump providing a base pressure of 0.01 Pa. Due to the condensable nature of solid

propellants, turbopumps are not a feasible choice since any condensation onto the blades can lead to failure of the pumping system. The ambient pressure in the vacuum chamber is measured with a pirani gauge and an ion gauge. The vacuum chamber, pumps and instrumentation are shown in Figure 6.

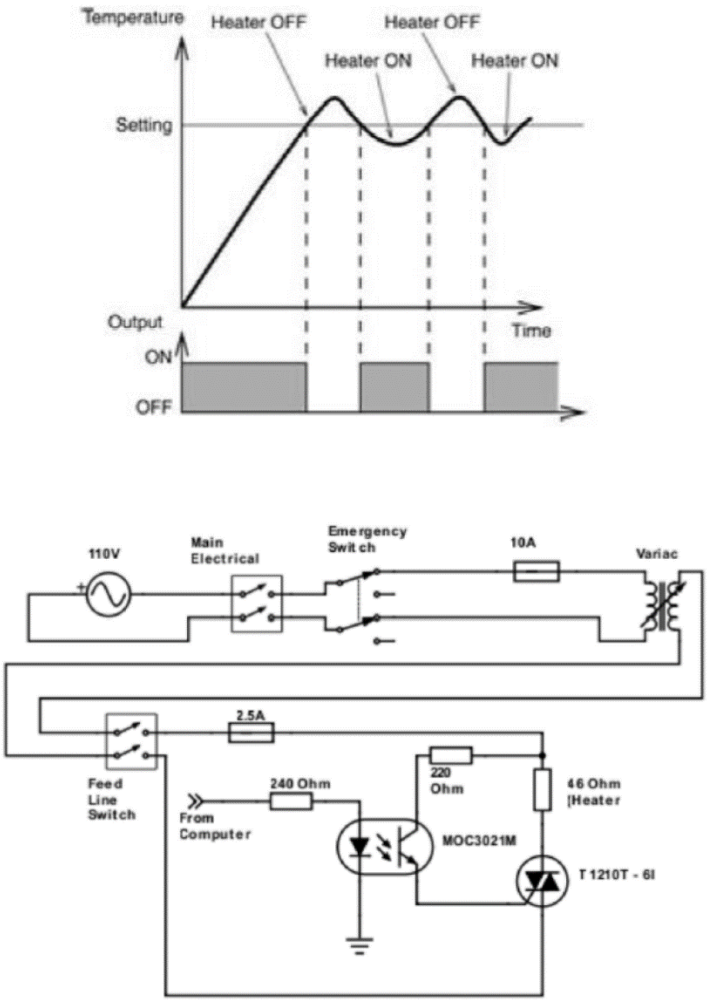

Figure 5: ON/OFF control behaviour and control circuit schematic [17]

4. INVESTIGATION OF THERMAL RESPONSE

To efficiently control sublimation, the surface temperature of the zinc slug must be known. Since the thermocouple is not located on the outer surface of the propellant slug which undergoes sublimation, but rather inside the cartridge heater in close contact with the heating element, the transient and steady-state temperature difference between the location of the built-in thermocouple and the surface of the zinc was experimentally determined as a function of time and for different operating conditions. The steady-state difference between the measured temperature of the cartridge heater built-in thermocouple and the cartridge heater sheath thermocouple was found to be 10^0C. This is a measure of thermal conduction through the oxide

Figure 6: "Dirty" Vacuum chamber and pumps

layer within the cartridge heater which can differ on other heater models. Heat change on the heater sheath surface is almost instantaneous and synchronous to the built-in thermocouple reading. A test was performed with the cartridge heater inside the zinc slug in air. This was to observe the temperature difference between the zinc surface and the cartridge heater thermocouple. A $\Delta T=30^0$ C can be seen in Figure 7. Tank surface temperatures are also 10 degrees behind the slug. This analysis was done to highlight any problems in heat transfer from an early stage but to also benchmark the performance for future iterations of the PSDS.

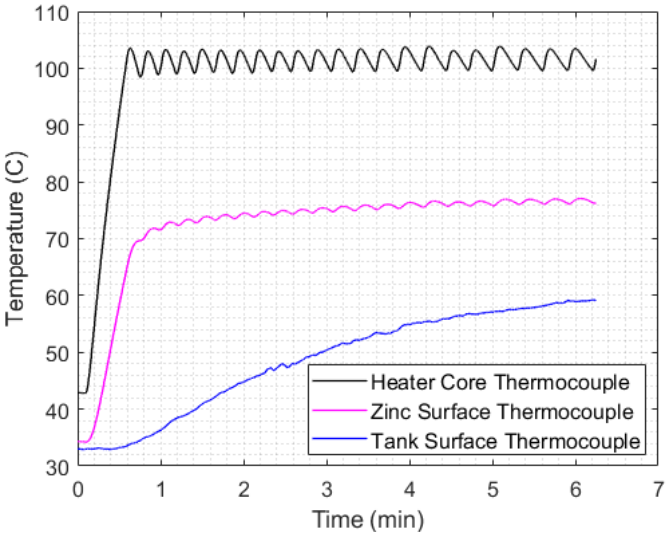

Figure 7: In air calibration run of the full assembly at 100^0 C

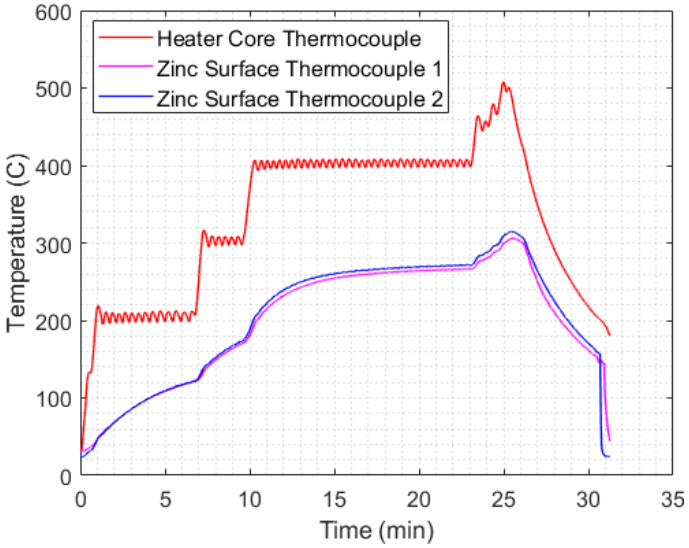

Figure 8: Vacuum calibration run of the full assembly up to 500^0 C

The final and most important test was performed in vacuum at a much higher temperature. The target was 500^0 C and the full assembly was tested. Two thermocouples were secured on the zinc slug on different sides of the surface to check heating uniformity across the annular shape. The temperature history recorded in the test can be seen in Figure 8 with the two thermocouples on opposite sides labelled thermocouple 1 and 2. In vacuum, the temperature difference between the core cartridge heater thermocouple and the zinc slug surface is large, close to ΔT=135-145^0 C. However, surface contact does not seem to be an issue as the two thermocouples used were reading similar values within their manufacture error. In this test, the tank itself only reached 100^0 C which was much lower than the expected temperature. This experiment showed two important aspects of the setup. Firstly, the controllability of the PSDS is excellent as the oscillations inherent in the ON/OFF control are dampened on the surface into an almost constant target temperature. The issue lies in accurately mapping the temperature on the surface to the reading from the cartridge heater thermocouple. Secondly, the time required to reach the target temperature is dependent on the method of heating. In this case, an incremental approach was taken where the temperature was increase by 100^0 C every few minutes. This was to ensure the surface of the slug in contact with the cartridge heater does not melt. As a result, the surface reached a steady temperature after 15 minutes. This aspect was addressed during testing by the introduction of a pre-heat step.

5. OPERATION OF THE EXPERIMENT

For each test, the PSDS was disassembled, cleaned and weighed on an individual component basis with an error of $\pm$1 mg. The inside of the tank with the zinc slug mounted on the cartridge heater can be seen in Figure 9. After reassembly, the power was cycled up to 100^0 C to verify the electronics and then the vacuum chamber was pumped down for testing. The sublimation rate was measured for a range of heater powers beginning with the lowest power and progressively increasing the heater power until sublimation with minimal condensation was achieved. Temperature control was done manually by changing the target setpoint via the LabVIEW interface. Operational voltages have been manually adjusted via the variac during the tests from an initial 110 V at warm up, down to 40 V at steady-state operation to stabilize the error for a certain temperature. Overall, the heater temperature error was within $\pm$2.5^0 C with an estimated $\pm$1.5^0 C at the surface of the zinc slug. To observe condensation and to account precisely the mass of zinc which sublimated, the anode heater was powered down turning the tank walls effectively into a cold trap. The system integrity and response through the warm-up cycle was first verified. Heater power was gradually increased until the first sign of zinc mass loss was recorded marking the lower temperature bound of the sublimation window.

Figure 9: PSDS before testing

6. RESULTS

The results from the PSDS sublimation tests are presented.

6.1. Slug Surface Effect on Sublimation

Traces of condensation could be found on the tank from 277-280^0 C after 60 minutes, adding up to 3 mg of zinc lost from the slug. A small zinc deposit can be seen in Figure 10.

Gradually increasing the temperature for the same

Figure 10: Zinc formations inside the stainless-steel tank; 60-minute; 0.01 SCCM (0.0008 mg/s); 280^0 C.

amount of time in the next few tests had an unexpected effect. For a run at 282^0 C 3 mg of zinc sublimated, at 287^0 C 4 mg sublimated and finally for a run at 292^0 C only 3 mg of zinc were produced. This behaviour seemed unexpected. Upon closer inspection it was found that the surface of the zinc slug was in poor condition. The difference between a freshly machined slug and the state of the tested one can be seen in Figure 11. It is suspected that the slug surfaces undergo either a possible chemical reaction once the vacuum chamber is brought back to atmospheric pressure or an emissivity change occurs increasing heat losses and reducing the temperature. Furthermore, in this case, it was suspected that oil deposition caused by an accidental backflow of vapor from the diffusion pump worsened the effect. A freshly machined slug was used as a replacement with the same specifications.

Figure 11: Surface finish on the tested zinc slug and the replacement slug in the background.

After the slug was replaced, a 292^0 C, 60-minute test yielded roughly 100 mg of zinc equivalent to 0.55 SCCM (0.0275 mg/s).

A further back-to-back test with this slug aimed at repeating the initial 100 mg sublimated mass result using the same procedure and temperature yielded only 10 mg of zinc at 292^0 C. This showed that the issue identified previously relating to the surface was not accidental. In this case the surface change is more drastic with heavy pitting. Figure 12 shows the zinc slug after testing displaying a crystalline structure.

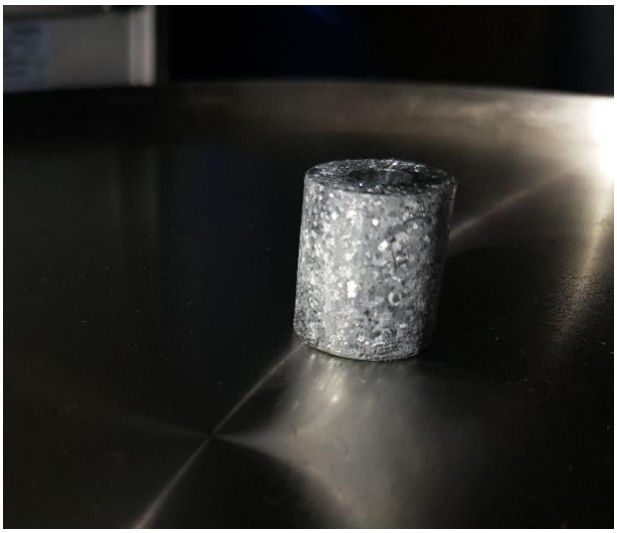

Figure 12: Surface finish of the zinc slug after a successful test.

It was speculated that the slug surface does not reach the target temperature when the test is started due to an emissivity change and a higher heat loss rate. A 30-minute period before the start of the test was introduced where the temperature is set higher than the target value by 50-80 ^{0} C. This is done in accordance with slopes obtained from the initial thermal response investigation data to give enough time and a better temperature gradient to the zinc slug. This step improved the performance and flow rates of up to 6.09 SCCM (0.2961 mg/s) have been recorded at 312^0 C in a 60-minute test. Furthermore, the result was repeated in a back-to-back test with slightly lower flow rates due to small differences in the heat up procedure.

The temperature profile recorded with the cartridge thermocouple over time for a 4.11 SCCM (0.2002 mg/s) test at 310 ^{0} C with the inclusion of the 30-minute pre-heat interval is shown in Figure 13. Adjustment of the heater power and target temperature have been done manually via the control software and due to the nature of the ON/OFF control small variations are present in

successive runs. However, similar flow rates have been obtained within 0.2 SCCM (0.001 mg/s) of each other.

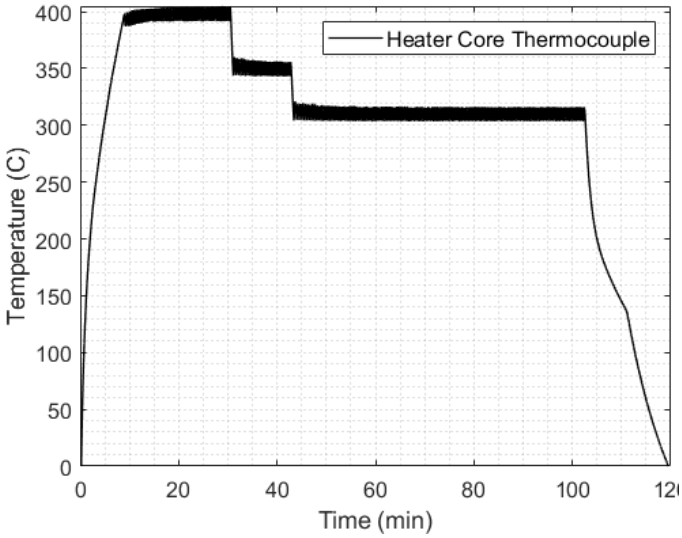

Figure 13: Cartridge heater core temperature (calibrated) vs time history for a 4.11 SCCM (0.2002 mg/s) run.

Although the pre-heat step mitigates to a certain degree the issues described previously regarding the lower sublimation rate in successive tests, more experiments are required to identify the issue. It is of particular importance to verify if the process is of an emissive nature or a chemical one specific only to zinc as a fully functional PSDS needs to be robust, predictable and reliable in functionality.

6.2. Higher Flow Rates and Hall Thruster Suitability

Flow rates of up to 6.09 SCCM (0.2961 mg/s) have been produced using the refined testing sequence. The variation in condensed zinc quantities can be seen in Figures 14 and 15. For this experiment, the lower end of the sublimation range was targeted to demonstrate accurate control and repeatability as an improvement from the previous iteration. The PSDS can operate throughout the sublimation interval of zinc (up to the melting point $419.5^0\ C$) and thus higher flow rates can be reached with a similar input power.

6.3. Input Power Requirements

The required power input ranged from 110 W at the beginning of the warm-up sequence and was manually and gradually decreased down to 40-60 W during steady state operation. In the next prototype, radiative losses will be further reduced through layered shielding which is expected to decrease the power consumption. It is expected that the finalized PSDS will operate under a more optimized power regime using PID control rather than ON/OFF switching.

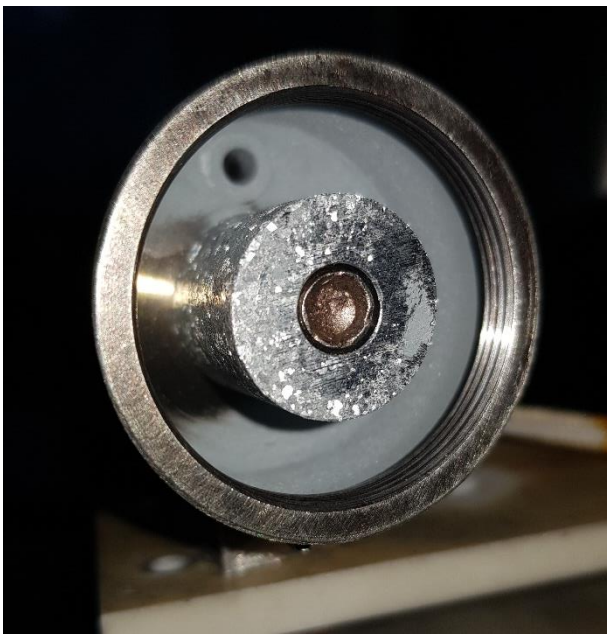

Figure 14: Zinc condensation observed after the test; 60-minute; 0.56 SCCM (0.0275 mg/s); $292^0\ C$.

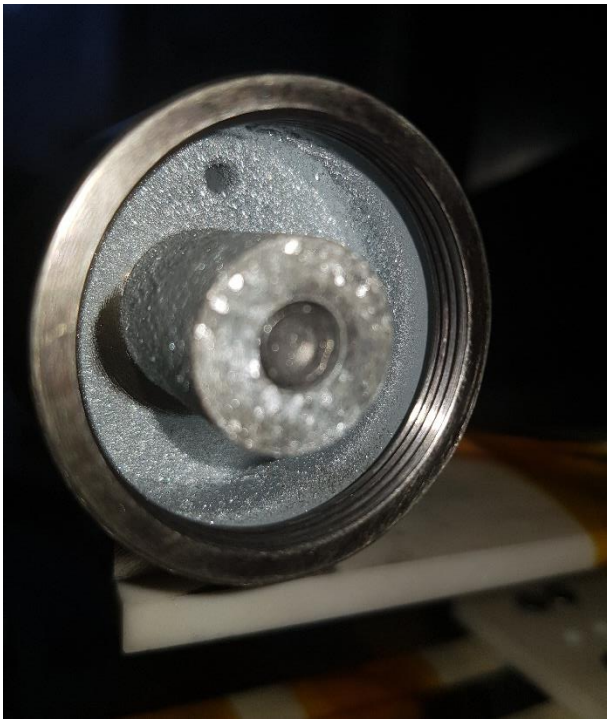

Figure 15: Zinc condensation observed after the test; 60-minute; 6.09 SCCM (0.2961 mg/s); $312^0\ C$.

7. DISCUSSION

The PSDS successfully produced a zinc flow rate of up to 0.2961 mg/s, sufficient to power a small Hall thruster, at an average input power of 75 W which is roughly 65% less power compared to previous designs [19]. The results validate the heating method chosen and the prospect of accurate control with a more refined design. Low flow rates between 0.5 SCCM (0.0275 mg/s) and 6.09 SCCM (0.2961 mg/s) were achieved and sustained and can be

further improved upon with a more detailed temperature calibration map and control mechanism. The PSDS is fully capable of operating at higher flow rates up to 20 mg/s close to the melting point of zinc ($419.5^0\ C$) with a constant 110 W power input. The results from the experiments overlayed onto an ideal sublimation rate for zinc can be seen in Figure 16 and 17. It also includes the corrected flow rate with a fitted $\eta = 0.7$. This large value of η suggests an efficient heat transfer mechanism where most of the heat is used to phase transition the solid.

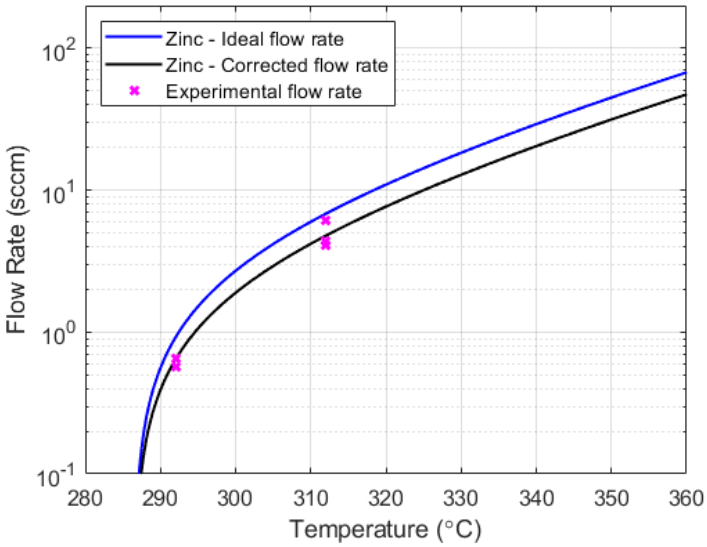

Figure 16: Theoretical, corrected $\eta = 0.7$ and experimental flow rate ($\dot{m}$) in SCCM vs temperature (T) for zinc. $P_c = 0.1\ Pa$

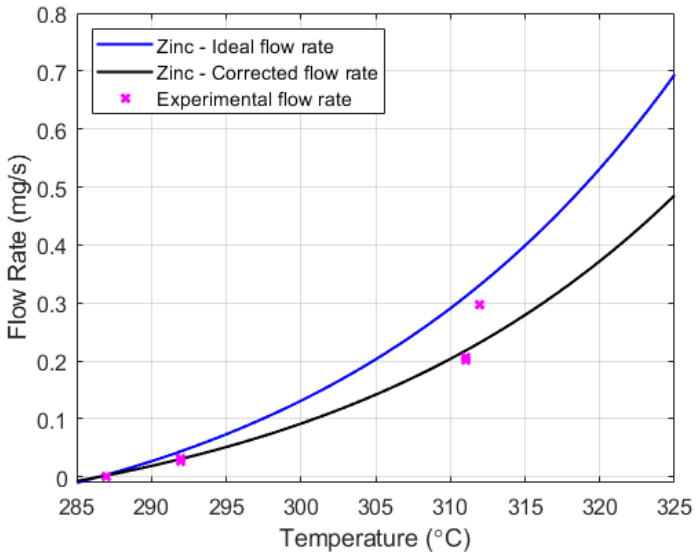

Figure 17: Theoretical, corrected $\eta = 0.7$ and experimental flow rate ($\dot{m}$) in mg/s vs temperature (T) for zinc. $P_c = 0.1\ Pa$

7.1. Condensation

Condensation is an important aspect in solid propellant usage as it can affect critical subsystems in a spacecraft. In this iteration of the PSDS, condensation was encouraged to observe the phenomenon and a few important findings were uncovered.

Figure 18: Zinc deposit peeling off the stainless-steel tank.

First, it was found that the zinc crystalline deposits are only superficially attached to the stainless-steel surface of the tank and can be peeled off easily. This behaviour can be seen in Figure 18 and it is unlike what was seen in the first prototype experiments where the crystalline formations protruded heavily while being securely attached to the stainless-steel casing. This finding is important as it points to the possibility of a surface coating that will inhibit zinc deposition. Experiments with zinc

and copper separation [17] also support this idea. It is important to find a solution to condensation contamination when the wetted surfaces cannot be heated above the sublimation temperature. Thus, the prospect of a potential inhibiting coating is appealing and will be explored in further experiments.

Secondly, it was found that the 22.25 mm feed line had only superficial condensation evidence localized at the connection point with the tank. With roughly 20% of the mass of zinc leaving the tank even with the anode heater off (tank walls acting as a cold trap), it is possible to construct a propellant tank that requires no feed line heating if short direct distribution is ensured via the anode connection.

This significantly reduces the input power required to operate the PSDS especially in propellants that require a higher temperature for sufficient vapor pressure. This concept was integrated in the third PSDS iteration.

8. CONCLUSION AND FUTURE WORK

8.1. Conclusions

Building upon the results of previous experiments, progress has been made towards the construction of a dedicated metallic propellant storage and delivery system for use with Hall thrusters.

The ideal flow rates from a modified Hertz-Knudsen theoretical model agree with experimental data showing a heater efficiency of $\eta = 0.7$ for the heating method used herein. The theoretical prediction of a high flow rate sensitivity to temperature was confirmed in experiments with mass flow variation up to 0.5 SCCM (0.0243 mg/s) for temperature changes of 1-3^0 C.

Accurate thermal control was achieved to within 0.5 SCCM (0.0243 mg/s) and operational power was 65% lower than that observed in the first prototype [19]. This represents a major improvement over previous PSDS versions that operated at an excess of 220 W input power producing highly variable flow rates over 15 SCCM (0.7291 mg/s) with no correlation between temperature and flow rate.

With an average input power of 75 W, zinc flow rates between 0.5 SCCM (0.0275 mg/s) and 6.09 SCCM (0.2961 mg/s) were sustained for a duration of 60 minutes. Considering the operational window of 4 SCCM (0.39 mg/s xenon) to 10 SCCM (0.97 mg/s xenon) for a typical 100-200 W Hall Thruster, the PSDS was demonstrated to achieve the required flow rate to sustain such a thruster with a steady state heater power input of 40 W. Higher flowrates up to 20 mg/s can be achieved with this PSDS design with a constant heater input of 110 W, the limiting factor being the melting point of zinc.

8.2. Future Work

Observations of the condensation behaviour within the feed line suggest the possibility of designing a PSDS without an additional feed line heater. The design phase of a refined PSDS (prototype 3) along with an improved control system was concluded. The performance of this refined design will be measured prior to integration with a Hall thruster. Performance measurements of the Hall thruster operating on zinc will be compared with performance measurements for the same thruster operating on xenon.

9. ACKNOWLEDGEMENTS

The authors would like to thank OHB Sweden for the continued support of this research.

10. REFERENCES

[1] A. Lorand, O. B. Duchemin, S. Zurbach, D. L. E. Mehaute, and N. Cornu, “Alternate propellants for PPS_Hall-Effect Plasma Thruster.pdf,” 2013.

[2] J. Szabo, M. Robin, J. Duggan, and R. R. Hofer, “Light Metal Propellant Hall Thrusters,” *31st Int. Electr. Propuls. Conf.*, pp. 2009–138, 2009.

[3] C. B. Alcock, V. P. Itkin, and M. K. Horrigan, “Vapour pressure equations for the metallic elements: 298-2500k,” *Can. Metall. Q.*, vol. 23, no. 3, pp. 309–313, 1984, doi: 10.1179/cmq.1984.23.3.309.

[4] D. A. Herman and K. G. Unfried, “Xenon Acquisition Strategies for High-Power Electric Propulsion NASA Missions,” *7th JANNAF SPS Subcomm. Meet.*, 2015.

[5] F. Paganucci *et al.*, “Progress on the Development of an Iodine-fed Hall Effect Thruster,” *35*, pp. 2017–418, 2019.

[6] T. Andreussi *et al.*, “Identification, Evaluation and Testing of Alternative Propellants for Hall Effect Thrusters,” *35th Int. Electr. Propuls. Conf.*, p. IEPC--2017--380, 2017,

[7] A. Shabshelowitz, A. D. Gallimore, and P. Y. Peterson, “Performance of a helicon hall thruster operating with xenon, argon, and nitrogen,” *48th AIAA/ASME/SAE/ASEE Jt. Propuls. Conf. Exhib. 2012*, no. August, pp. 1–11, 2012, doi: 10.2514/6.2012-4336.

[8] J. Szabo, M. Robin, J. Duggan, and R. R. Hofer, “Light Metal Propellant Hall Thrusters,” *31st Int. Electr. Propuls. Conf.*, no. April, pp. 2009–2138, 2009.

[9] D. Rafalskyi and A. Aanesland, “Development and Testing of the NPT30-I2 Iodine Ion Thruster,” *36th Int. Electr. Propuls. Conf.*, no. March 2020, pp. 1–11, 2019, doi: 10.6084/m9.figshare.11931363.

[10] J. Szabo, M. Robin, and V. Hruby, “Bismuth Vapor Hall Effect Thruster Performance and

Plume Experiments," *Iepc2017*, pp. 1–13, 2017,
[11] S. O. Tverdokhlebov, A. V. Semenkin, and J. E. Polk, "Bismuth propellant option for very high power TAL thruster," *40th AIAA Aerosp. Sci. Meet. Exhib.*, no. January, 2002, doi: 10.2514/6.2002-348.
[12] A. Kieckhafer and L. B. King, "Energetics of propellant options for high-power hall thrusters," *J. Propuls. Power*, vol. 23, no. 1, pp. 21–26, 2007, doi: 10.2514/1.16376.
[13] M. Hopkins and L. B. King, "Performance comparison between a Magnesium-and Xenon-fueled 2 kW hall thruster," *50th AIAA/ASME/SAE/ASEE Jt. Propuls. Conf. 2014*, pp. 1–10, 2014, doi: 10.2514/6.2014-3818.
[14] J. M. Makela, R. L. Washeleski, D. R. Massey, L. B. King, and M. A. Hopkins, "Development of a magnesium and zinc hall-effect thruster," *J. Propuls. Power*, vol. 26, no. 5, pp. 1029–1035, 2010, doi: 10.2514/1.47410.
[15] M. A. Hopkins and L. B. King, "Magnesium hall thruster with active thermal mass flow control," *J. Propuls. Power*, vol. 30, no. 3, pp. 637–644, 2014, doi: 10.2514/1.B34888.
[16] J. Szabo, M. Robin, J. Duggan, and R. R. Hofer, "Light Metal Propellant Hall Thrusters," *31st Int. Electr. Propuls. Conf.*, no. April, pp. 2009–2138, 2009.
[17] L. Zhan, Z. Qiu, and Z. Xu, "Separating zinc from copper and zinc mixed particles using vacuum sublimation," *Sep. Purif. Technol.*, vol. 68, no. 3, pp. 397–402, 2009, doi: 10.1016/j.seppur.2009.06.009.
[18] F. Paganucci, D. Pedrini, L. Bernazzani, A. Ceccarini, and M. Saravia, "Development of an Iodine Propellant Feeding System for Electric Propulsion," no. 4, *Space Propulsion Conference* 2016.
[19] S. Dworski, J. Martin, C. Ryan, E. Dyer, and U. Kingdom, "The operation of a low-power cylindrical Hall thruster with zinc as the propellant," *36th Int. Electr. Propuls. Conf.* pp. 1–20, 2019.